Benchmark Results for Hydrogen Atom Transfer Between Carbon Centers and Validation of Electronic Structure Methods for Bond Energies and Barrier Heights

Agnieszka Dybala-Defratyka,[†,*] Piotr Paneth,[†,*] Jingzhi Pu,[‡,*] and Donald G. Truhlar[‡,*]

[†] Institute of Applied Radiation Chemistry, Technical University of Lodz, Zeromskiego 116, 90-924 Lodz, Poland

[‡] Department of Chemistry and Supercomputer Institute, University of Minnesota, 207 Pleasant St. SE, Minneapolis, Minnesota 55455-0431, USA

Abstract.

First we report benchmark high-level calculations for the barrier heights of five degenerate and nearly degenerate rearrangements ($CH_3^\bullet + CH_4$ or C_2H_6, $C_2H_5^\bullet + CH_4$ or C_2H_6, and $n\text{-}C_3H_7^\bullet + n\text{-}C_3H_8$) involving hydrogen transfer between hydrocarbon fragments. Then the performance of eleven existing and five new semiempirical methods based on neglect of diatomic differential overlap (NDDO) and intermediate neglect of differential overlap (INDO) is evaluated by comparing their predictions to those of the more accurate levels. All methods are additionally tested against a representative test suite of reactive barrier height and a representative test suite of bond energies. Two new NDDO methods, with one Gaussian function parametrized for reactions involving the transfer of hydrogen atoms between carbon centers, were developed to provide both accurate barrier heights and transition state geometries. The results show that the energetic barriers for transfer of hydrogen between carbon centers calculated by one of the existing NDDO levels, in particular Austin Model 1 (AM1), and by these two new methods, denoted AM1-CHC-SRP and PM3-CHC-SRP, agree well with the more accurate results and in particular have mean unsigned errors of only 1.9, 1.4, and 0.7 kcal/mol, respectively, and give reasonable transition state geometries, whereas 13 other NDDO and INDO methods (in particular PM3, PM3tm, PM3-AHR, PM3-NHR, PM3-3H2, PM5, MNDO, MNDO/d, MNDOC, SAM1, MSINDO, PDDG/PM3, PDDG/MNDO) that are tested have mean unsigned errors of $3.5 - 34$ kcal/mol or qualitatively incorrect transition state geometries for such transfers. Another interesting finding of this study is that hybrid density functional theory methods do not agree with high-level explicitly correlated methods for the trend in barrier height when methyl is changed successively to ethyl and n-propyl in the degenerate rearrangements. This indicates that they make different predictions about trends in the intrinsic barrier height parameter of Marcus theory and indicates that the

intrinsic barrier heights are very sensitive to approximations in the treatment of exchange and correlation.

1. Introduction

Proton, hydrogen atom, and hydride transfer reactions are of general importance in many biological processes, e.g., proton transfer across membranes, functional isomerizations of intermediary metabolites, or the transfer of reducing equivalents between enzyme substrates and cofactors. In enzymatic reactions, acid/base catalysis often involves proton movement, whereas redox catalysis often involves transfer of hydride; however, a significant number of enzymatic reactions occur by homolysis of a substrate carbon-hydrogen bond and subsequent formation of radicals, and this involves hydrogen atom transfer. Adequate theoretical treatment of these reactions becomes essential in understanding and explaining biological catalysis at the molecular level. The most common tool used in the description of enzyme catalysis and most other chemical reactions is transition state theory (TST).[1,2] In order to be capable of explaining the experimental findings for proton, hydride, or hydrogen atom transfer reactions, TST should include a transmission coefficient that accounts for quantum mechanical tunneling, which allows particles to penetrate into classically forbidden regions. Recent research has provided increasing evidence for the importance of hydrogen tunneling in enzymes under physiological conditions.[2-4] New techniques that combine the capability of quantum mechanics for describing bond rearrangements and electronic polarization with the computational speed of molecular mechanics (such as combined QM/MM methods) are especially promising for generating the potential energy surfaces needed for TST and tunneling calculations, and they have increased our ability to study mechanisms of enzymatic reactions.[2] Although one can expect that hybrid density functional theory[5,6] will ultimately be the QM method of choice, the size and complexity of protein systems means that there is also considerable interest in less expensive QM methods such as semiempirical molecular orbital theory along the lines of the popular AM1[7] and PM3[8] models.

Kinetic isotope effects are very important for disentangle reaction mechanisms, and they depend strongly on the changes of force constants around the isotopic atom(s); therefore it is important to obtain reliable geometries of the reactants and transition states. Tunneling, on the other hand, is very sensitive to the energetic profile along the reaction coordinate; thus the correct activation energy, barrier shape, and exo/endothermicity are necessary. In calculations of KIEs with tunneling it is therefore important to have accurate calculations of the geometries of reacting species and of the reaction energetics. In particular, it is important to ask whether less expensive methods predict accurate geometries, barrier heights, vibrational frequencies, and barrier widths, since all of these properties are important for calculating kinetic isotope effects (KIEs) and also for studying the involvement of quantum tunneling in reaction dynamics. Although we have emphasized biological chemistry in this introduction, similar questions arise in treating other complex phenomena such as reactions on the surfaces of metals (and other heterogeneous catalysts) and nanoparticles.[9]

A primary specific motivation for the present study is the hydrogen transfer reaction catalyzed by methylmalonyl-CoA mutase (MMCM).[4,10] The presence of coenzyme B_{12} and the radical species makes the treatment of this system very demanding and requires suitable and reliable methods at both the quantum mechanical and molecular mechanical levels of the QM/MM combination. Suitable models of the active site comprising important residues and large molecules of the reactant (MCoA) and the coenzyme (B_{12}) contain far too many (>100) atoms to be treated at a high QM level in free energy simulations. This forces one to choose a suitable level of calculation from among the less expensive alternatives, such as the semiempirical AM1 and PM3 methods. Our goal is to test whether there is a method that represents a useful compromise between the accuracy of high-level quantum mechanical calculations and the

affordability of simplified methods for such large molecular systems. Therefore we center attention on semiempirical methods based on neglect of differential overlap (NDO), since such method have been shown previously[11] to provide reasonable accuracy with low cost for many systems.

Here we present a validation study designed to evaluate the performance of affordable semiempirical methods with respect to the height of the energetic barrier for hydrogen atom transfer reactions at carbon centers and with respect to saddle point geometries for such processes; we consider both existing affordable methods and also new ones developed in this article. Four small systems have been studied, namely $CH_3^\bullet + CH_4$, $C_2H_5^\bullet + C_2H_6$, $C_3H_7^\bullet + C_3H_8$, and $CH_3^\bullet + C_2H_6 \leftrightarrow C_2H_5^\bullet + CH_4$. Both geometries and energetics obtained at inexpensive semiempirical levels are compared to those calculated by high-level calculations. Although these are obvious prototype systems that allow high-end calculations, no systematic studies were available performed thus far. Thus our study consists of three parts. In the first part we have made an attempt to find the correct energetic barriers and geometries of the saddle points for the H transfers at the most advanced theory levels presently available. In the second part we tested whether inexpensive molecular orbital theories can reproduce the correct results. This includes both ten previous semiempirical methods and five new ones designed in various ways to improve performance. In the third part we systematically test all 15 semiempirical molecular orbital methods against broader test sets of barrier heights and atomization energies.

2. Methods

Energetic barriers have been calculated using both single-point methods and methods that include full geometry optimization. The former are denoted X//Y, where the energy is calculated at the higher level X at the single geometry obtained by an optimization at lower level Y. The

methods used for geometry optimization include the Hartee-Fock (HF) method,[12] Møller-Plesset second order (MP2) perturbation theory,[13] two hybrid density functional methods: MPW1K[6] and B3LYP,[5] two multi-coefficient correlation methods (MCCMs): multi-coefficient Gaussian-3, version 3 (MCG3/3)[14,15] and multi-coefficient quadratic configuration interaction with single and double excitations, version 3 (MC-QCISD/3),[15,16] and the scaling all correlation method, version 3 (SAC/3).[15,17] For single point calculations we have used Gaussian-3 based on scaling[18] (G3S), reduced-order extended G3S[19] [G3SX(MP3)], and four available complete basis set (CBS) models, namely: CBS-APNO,[20] CBS-QB3,[20,21] CBS-Q[21], and CBS-4M.[22] The basis sets employed for ab initio methods are 3-21G(d),[23] 6-31G(d),[24] and 6-31+G(d,p).[24] For DFT calculations we have used 6-31+G(d,p)[24] and 6-31G(2df,p)[25] basis sets. Moreover, since MPW1K method proved previously to be the most satisfactory hybrid DFT method for kinetics,[16,26,27] we also tested this method with the MIDI!,[28] MIDIY+,[27] and MG3S[29a] basis sets. For systems containing only first row elements, such as the hydrocarbons in the present study, the MG3S basis set is identical to 6-311+G(2df,2p), in which the diffuse function on hydrogens has been removed from the 6-311++G(2df,2p) basis set.[29b]

The radical species have doublet electronic states and were treated with the UHF method[12b] and unrestricted correlated methods. All single-point calculations were preformed using the *Gaussian98* program.[30] The MCCM calculations were performed with the MULTILEVEL 3.0 program.[31] The spin-orbit contribution to the energy is zero for the present systems.[32] The MC-QCISD and MCG3 calculations were performed with version 3m coefficients.[15] The calculations using some of the more expensive methods were performed only for the smaller system.

The NDO methods tested in the present study include Austin Model 1 (AM1)[7] and Parametrized Model 3 (PM3)[8] as implemented in the MOPAC 5.09mn program[33] (the parameters are the same as in MOPAC 5 and MOPAC 6), PM3 for transition metals (PM3tm) as implemented in the SPARTAN package,[34] PM5[35] as implemented in MOPAC2002,[36] Semi-Ab-initio Model 1 (SAM1),[37] MNDO,[38] MNDO/d,[39] and MNDOC[40] as implemented in AMPAC,[41] Modified Symmetrically orthogonal Intermediate Neglect of Differential Overlap (MSINDO)[42] as implemented in MSINDO 2.6[43], and two Pairwise Distance Directed Gaussian (PDDG) methods,[44] namely PDDG/PM3 and PM3/MNDO, as implemented in a modified MOPAC 6.[45] The MNDO, MNDO/d, MNDOC, AM1, PM3, PM3tm, PM5, SAM1, PDDG/PM3, and PDDG/MNDO methods are based on Neglect of Diatomic Differential Overlap (NDDO).[46] The PM3tm method differs from PM3 in that it includes d-orbitals for metal atoms and second row atoms like sulfur and also in that it contains an additional energy term, which prevents hydrogen atoms from coming too close together; therefore it presents a particularly interesting method to be tested on hydrogen transfer reactions. SAM1 is like AM1 except that the parametric function used to estimate electron repulsion integrals in AM1 is replaced by directly calculated electron repulsion integrals (with an STO-3G basis set) multiplied by a parametric scaling function; in addition, the number of Gaussian correction functions in the core repulsion is reduced. MSINDO is based on Intermediate Neglect of Differential Overlap (INDO).[47] In addition to testing these eleven pre-existing methods, we also develop and test five new methods (PM3-AHR, PM3-NHR, PM3-3H2, PM3-CHC-SRP, and AM1-CHC-SRP), which are explained below. Of the 16 methods tested, MNDO/d, MSINDO, and PM3tm include d functions for second row atoms, and the other 14 methods include only s and p functions for all atoms involved in this paper.

3. Results and Discussion

    3-1. Energetics. First, to evaluate the general accuracy of the methods used in the present study, we calculate the mean unsigned error (MUE) for each method over a representative data set containing six barrier heights (BH6) and six atomization energies (AE6).[48] The BH6 and AE6 benchmarks have been shown to be representative of the performance of electronic structure methods on a larger data set with 44 reaction barrier heights and 109 atomization energies.[48] Because some of the methods are only available for the first row, we also calculate MUEs based on a subset of the representative data set which only contains hydrogen and first row elements (in particular C and O). The resulting subsets for systems only involving hydrogen and first row elements have four barrier heights and three atomization energies and are therefore denoted BH4 and AE3 respectively. The MUEs against the representative benchmarks are tabulated in Table 1 as indications of the overall accuracy of each method in terms of their ability to predict barrier heights and bond energies. Note that the MUEs of AE6 and AE3 are expressed on a per bond basis, where triple bonds and double bonds are counted as a single bond. To do this we divide the mean error per molecule in these two sets by the average number of bonds per molecule, which is 4.83 for AE6 and 7.67 for AE3. Although we focus on MUEs in the article (except in the case when RMSE is used to optimize parameters), the root-mean-squared-error (RMSE) and mean-signed-error (MSE) for all methods tested against BH6, BH4, AE6, and AE3 benchmarks are available in the supporting information, also on a per bond basis. Table 1 forms a background for the more specific tests on reactions involving transfer of H between carbon centers, as considered next. In Table 1 (and the following two tables as well), the methods are grouped by their asymptotic scaling factors N^{α}, where N is the number of atoms, and α is in the range of $3 - 7$.[49] These scalings are based on the amount of work per iteration and do not take account of the fact

that the number of iterations tends to increase with system size; nevertheless they provide useful clues to affordability. Higher-level methods have higher α. In the first three tables the individual methods within each class with the same scaling are listed in the order of their accuracy for the BH6 data set.

Table 1

The energetic results for reactions in which hydrogen atoms are transferred between carbon centers are presented in Tables 2 and 3. Table 2 contains the barrier heights for degenerate rearrangement reactions $C_nH_{2n+1}^{\bullet} + C_nH_{2n+2}$ ($n = 1, 2, 3$). Table 3 gives the forward and reverse barrier height as well as the reaction energy for one unsymmetric hydrogen transfer reaction. In the cases of $C_2H_5^{\bullet} + C_2H_6$ and $C_3H_7^{\bullet} + C_3H_8$, results are shown for two saddle point conformations, *gauche* and *trans*. The energy difference between them is less than 0.1 kcal/mol, but both are given in the table.

Tables 2 and 3

The experimental activation energy is known only for the $CH_3^{\bullet} + CH_4$ system,[50] and it is equal to $14 - 15$ kcal/mol. This is consistent with the higher-level correlations in Table 1 since experimental activation energies tend to be within a few kcal/mol of the barrier height. Although there are no experimental activation energies for the higher analogs, considerable experience for nonsymmetric reactions shows that methane essentially always has a higher activation energy for hydrogen abstraction than the higher homologs. This is consistent with more reliable post-Hartree-Fock methods (the N^7 and N^6 methods) that are available for higher homologs in Table 1, which show that the classical barrier heights decrease by about $1.1 - 1.6$ kcal/mol in going from C_1 to C_2 and by another $0.5 - 1.2$ kcal/mol in going from C_2 to C_3. It is, disconcerting that the expected trend of decreasing barrier height with increasing fragment size for the H transfer

between symmetric fragments is not observed in the hybrid DFT calculations or most of the semiempirical calculations. In Marcus theory,[51-58] the barrier for the symmetric reactions, like $CH_3^\bullet + CH_4$ or $C_2H_5^\bullet + C_2H_6$, is called the intrinsic barrier height, and it has a simple interpretation in terms of the re-organization energy. The present calculations show that explicitly correlated wave functions predict a different trend than hybrid DFT for the variation of the intrinsic barrier height or the re-organization energy with changes in the molecular structure of the donor and the acceptor radicals.

The unsymmetric H transfer reaction $CH_3^\bullet + C_2H_6$ represents an interesting comparison to these symmetric reactions. As Tables 2 and 3 show, DFT calculations predict the relative barrier heights between symmetric and unsymmetric reactions with the correct pattern, i.e., $CH_3^\bullet + CH_4 > CH_3^\bullet + C_2H_6$ and $CH_3^\bullet + C_2H_6 < C_2H_5^\bullet + C_2H_6$.

As is well known, HF methods tend to overestimate the energetic barrier for hydrogen transfer reactions, a conclusion supported by the data available in the literature for similar systems.[59] Although unscaled MP2 calculations performed significantly better than the HF ones, they still seem to be quite far from the results of the higher-level methods. The inclusion of diffuse and polarization functions in the basis set was found to improve the energetic barrier significantly, but not nearly enough. However, perturbation theory methods with large basis sets are expensive and can be applied only to systems with a very small number of atoms.

G3S, G3SX(MP3), MCG3/3, and CBS-APNO are the most reliable methods considered in this article and therefore were used as important components of our consensus benchmarks for our comparison study. As can be seen they give values in excellent agreement with each other, with the first three differing from one another by only 0.2 kcal/mol. According to the results obtained using these three methods, the classical barrier height for $CH_3^\bullet + CH_4$, $C_2H_5^\bullet + C_2H_6$,

and $C_3H_7^{\bullet} + C_3H_8$ systems should be within the range of $17 - 18$, $16 - 17$, and $15.5 - 16.5$ kcal/mol, respectively, indicating as discussed above, a slight lowering of the barrier with the increase of the number of carbon atoms. Unfortunately usage of these methods is also limited to very small systems. Furthermore, the CBS-APNO method gives the surprisingly low result of 16.7 kcal/mol for the $CH_3^{\bullet} + CH_4$ barrier. Table S2 (see supporting information), however, shows that CBS-APNO does seem to systematically underestimate barrier heights, a result that was apparently not appreciated before.

Since accurate evaluation of the H-transfer energetics with regard to the kinetics was of particular interest, the MPW1K method, a method specifically parameterized for kinetics, was also used. Data in Tables 2 and 3 confirm the reaction barrier and energies.

In order to test the less expensive methods systematically, we computed a consensus barrier height for every reaction in Tables 2 and 3. We did this by averaging the best available G3, MCG3, CBS, MC-QCISD, and MPW1K values for that reaction. These values are in bold in Tables 2 and 3, and the consensus values of the barrier heights are in Table 4.

Table 4

Among the inexpensive semiempirical methods, the AM1 and PM3tm methods performed the best in this test. By producing results that are within $2 - 4$ kcal/mol of the values predicted by accurate calculations these two semiempirical methods are validated for studies of the energetics of H transfer between alkyl hydrocarbon fragments. Although they are often discredited as being unreliable for quantitative analysis (and they *are* unreliable except where validated for similar problems), they are sometimes the only tool available, especially in case of large systems; thus their good performance with regard to the present reaction barriers is very promising for their use within the QM/MM framework. Table 1 shows that the AM1 method retains its accuracy much

better than PM3tm when the barrier height test data is broadened from only CHC reactions to BH6 or BH4.

The AM1 method shows the same trend in barrier heights, as the alkyl chain is lengthened, as is seen for the benchmark methods, except that the value obtained for $CH_3^{\bullet} + CH_4$ is lower than the expected one by 4 kcal/mol

Within the family of PMx Hamiltonians, both PM3[9] and the newly developed PM5 parametrization[34] substantially underestimate the barrier heights for all the studied systems. The PM3tm method, on the other hand, yields good energetics and shows the same trend in activation barrier as obtained with the benchmark methods. While this parametrization was created with transition metals in mind, it contains an additional energy term preventing too close contact between hydrogen atoms. The additional energy term was motivated by the fact that the PM3 method leads to an artificial minimum for H-H interactions at about $1.7 - 1.8$ Å[60] due to the inclusion of two closely centered Gaussian-functions (in the core repulsion) with opposite sign; there were attempts to correct this situation by modifying the Gaussian-functions.[61] In PM3tm a repulsive term between non-bonded hydrogens has been added as a general correction term; the only published explanation of this term that we could find gives it as[62]

$$G(HH) = (0.15\text{eV})e^{-(10.0\text{Å}^{-2})(r-1.7\text{Å})^2} \tag{1}$$

where r is the distance between two non-bonded hydrogen atoms. Apparently this is an important contribution in the case of systems studied here. Unfortunately, the method used to determine which hydrogen pairs are "non-bonded" and the exact form of the correction term used in the PM3tm implementation in SPARTAN have not been reported by the developers of the method, and repeated requests to the distributor of this program to obtain the official version of the correction did not yield any information. Furthermore, we have found that in molecules containing nearby

hydrogens, such as H_2, CH_3, and CH_4, the results that SPARTAN yields for PM3tm are the same as the results for PM3. In light of the empirical success of PM3tm and the uncertainty about the added term that seems to be responsible for that success, we embarked on a program to (i) figure out exactly what PM3tm does and (ii) optimize such a repulsion term on our own, and the results of these studies are described next.

To examine the form of the Gaussian function used by PM3tm, we first implemented eq. (1) along with the PM3 model in MOPAC 5.09mn.[32] To illustrate the effect of the definition of the "nonbonded" hydrogens, we tested two possibilities. In the first, we simply include all hydrogen pairs in the Gaussian terms. We label this method as PM3-AHR (PM3 with all hydrogen repulsions). The second method employs the definition of nonbondedness that we inferred to be the one used by SPARTAN. SPARTAN's definition can be motivated as follows. Because hydrogen has only one valence electron, there would be at most atom bonded to a hydrogen, if there is any, and this can be identified as the closest neighbor to the given hydrogen. With the atoms bonded to all hydrogens located, one can further identify 1–2 bonded hydrogens (the atom bonded to a hydrogen is also a hydrogen) and the 1–3 bonded hydrogens (hydrogen pairs bonded to the same atom, i.e., two hydrogens gemnial to each other). The HH pairs other than 1–2 and 1–3 bonded pairs are considered as nonbonded. Following this simple algorithm, we can screen out all 1–2 and 1–3 bonded hydrogen pairs from the Gaussian term, and only retain the repulsions between 1–4 and further apart HH pairs in eq. (1), and the resulting method is denoted PM3-NHR (PM3 with nonbonded hydrogen repulsions).

Table 2 shows that although PM3-AHR improves the barrier heights for the title reactions in the correct direction (PM3-AHR gives barrier heights of ~13 kcal/mol compared to ~11 kcal/mol in PM3), it does not quantitatively agree with the PM3tm barrier height (~17 kcal/mol). In fact,

for the unsymmetric hydrogen atom transfer reaction $CH_3^\bullet + C_2H_6$ (as shown in Table 3), PM3-AHR predicts quite different barrier heights and reaction energies than PM3tm. On the other hand, for the method with only nonbonded hydrogen repulsions included, we get excellent agreements with PM3tm; PM3-NHR reproduces PM3tm energetics results in Table 2 and Table 3 within 0.2 kcal/mol and 1 kcal/mol respectively. We also note that PM3-NHR predicts an asymmetric transition states for $C_nH_{2n+1}^\bullet + C_nH_{2n+2}$ (n = 1, 2, 3) as PM3tm does, while PM3-AHR does not have this distinguishing defect, and this will be discussed in more detail in Subsection 3-2.

In order to more fully test the usefulness of additional H-H repulsions to improve the performance of the PM3 model, we further optimized such terms in two ways using a genetic algorithm[63] (GA). In the first method, the PM3 energy was augmented by an empirical Gaussian-type repulsive term G(HH) between hydrogens of the form

$$G(HH) = Ae^{-[(r-r_0)^2 / \lambda^2]} \tag{2}$$

where A and λ represent the height and the width of the Gaussian function centered at r_0; r is the distance between two hydrogens. Note that we consider all hydrogen pairs in this model. The proposed Gaussian term was parameterized against a kinetics database that contains best estimates of the 23 reaction energies and the 46 reaction barrier heights for 23 gas-phase reactions; the data for 22 of these reactions are taken from previous work,[15] and the reaction of $CH_3^\bullet$ with CH_4 is also included, where the consensus barrier height of Table 4 was used as the best estimate. The values of the three parameters A, r_0 , and λ were obtained by minimizing the root-mean-squared-errors (RMSEs) over all 69 data in the database. The center of the Gaussian was optimized within the range 0.5 Å – 2.5 Å. We name this first model as PM3-3H2 (PM3 with

three parameters to improve H_2), because we find that for all practical purposes the optimized Gaussian in this method actually only affects the hydrogen molecule, as we will discuss below.

Next, using the approach of specific reaction parameters (SRP),[64] we reoptimized the parameters of eq. (2) for a smaller data set corresponding only to reactions transferring a hydrogen atom between carbon centers. Considering that one may make the geometries worse by optimizing the specific reaction parameters entirely on the basis of energies, here we use a combined criterion involving both energetics and geometries. In particular, the three Gaussian parameters were obtained by maximizing the following fitness function:

$$\text{Fitness} = -\left[\frac{1}{m}\sum_{i=1}^{m}\left(\frac{V_i - V_i^c}{V_0}\right)^2 + \frac{1}{n}\sum_{i=1}^{n}\left(\frac{R_{i,\text{C}-\text{H}} - R_{i,\text{C}-\text{H}}^c}{R_0}\right)^2 + \frac{1}{l}\sum_{i=1}^{l}\left(\frac{\theta_{i,\text{C}-\text{H}-\text{C}} - \theta_{i,\text{C}-\text{H}-\text{C}}^c}{\theta_0}\right)^2\right]^{\frac{1}{2}} \quad (3)$$

where V_i^c are the consensus reaction barrier heights listed in Table 4; $R_{i,\text{C}-\text{H}}^c$ and $\theta_{i,\text{C}-\text{H}-\text{C}}^c$ are the consensus values of the breaking and forming C–H bond distances and C–H–C angles involving the transferred hydrogen in the transition states listed in Table 12 (as we will discuss in the Subsection 3-2); V_0, R_0, and θ_0 are scaling parameters, and we use $V_0 = 1$ kcal/mol, $R_0 = 0.01$ Å, and $\theta_0 = 1$ degree in the present study; m, n, and l are numbers of the energies, bonds, and angles in the SRP training set, and furthermore $m = 5$, $n = 7$, $l = 6$. We will label this SRP model PM3-CHC-SRP (PM3 with specific reaction parameters for hydrogen atom transfer between C centers). The reason for examining an SRP method is to check whether the Gaussian term is useful for the specific range of reactions that we are particularly interested in.

Tables 5, 6, and 7

Table 5 shows the optimized values of the parameters of PM3-3H2 and PM3-CHC-SRP; the equivalent parameters used in PM3tm [as in eq. (1)] are also given for comparison. Barrier

heights and reaction energies for PM3, PM3-3H2, and PM3-CHC-SRP are presented in Table 6, and Table 7 contains RMSEs and mean-unsigned-errors (MUEs) of the PM3-3H2 and PM3-CHC-SRP compared to PM3. The HH repulsive Gaussian is forced to be centered at 0.764 Å in PM3-3H2, and the added Gaussian repulsions in this method decrease the RMSE of 69 data from 14.1 kcal/mol (PM3) to 11.3 kcal/mol (PM3-3H2), but the Gaussian term optimized for this model has a nonnegligible contribution to the energy only when two hydrogens are as close as in molecular H_2. Therefore the overall improvement in PM3-3H2 is almost entirely due to a better energetic description of H_2, and as shown it Table 6, the additional Gasussian in PM3-3H2 has significant effects only on reactions involving H_2. The optimized position of the Gaussian in PM3-3H2 is not directly related to the artificial HH well of the PM3 model at $1.7 - 1.8$ Å, and the PM3-3H2 Gaussian does not help to improve the barrier height for the prototype reaction $CH_3^\bullet$ + CH_4. We conclude that a general parametrization of eq. (2) does not provide a systematic improvement in barrier heights, and this is confirmed in Table 1. Table 1 also allows us to test whether including repulsions between all pairs of hydrogens, as in PM3-AHR and PM3-CHC-SRP has an adverse effect on atomization energies (since atomization involves the loss of a large number of 1–3 interactions among hydrogens). Table 1 shows that these methods make atomization energies only slightly worse for molecules with first row and second row atoms.

Since the PM3-CHC-SRP Gaussian has r_0 close to 1.7 Å, the artificial HH stabilization in PM3 is directly addressed, as are the barrier heights of specific interest in this paper. Although the overall performance on barriers (vs. BH6) of PM3-CHC-SRP is worse than PM3-3H2 and PM3 (see Table 1), the RMSE over the consensus barrier heights for CHC reactions is greatly reduced from 5.7 kcal/mol to 0.8 kcal/mol. Thus this method fulfills our objective in creating it. It is interesting that the optimized parameters in PM3-CHC-SRP are very close to the ones used in

PM3tm, and the improvements of barrier heights for the title reactions in both methods are quite significant.

Because AM1 also underestimates the barrier heights for CHC reactions as PM3, it is clear that an SRP improvement based on Gaussian repulsions between hydrogens would improve AM1 as well PM3. Therefore, we also parametrized a CHC SRP method for AM1 to maximize eq. (3), and we denote the corresponding method as AM1-CHC-SRP. The optimized Gaussian parameters in AM1-CHC-SRP are given in Table 5.

To evaluate the accuracy for kinetics of the semiempirical candidates (all NDDO and INDO methods that we tested), we tabulate the mean unsigned errors of all 16 NDO methods considered in this paper over the consensus barrier heights of CHC reactions and over the BH6 and BH4 benchmarks in Table 8. The methods are listed in the same order as in Tables 1 – 3.

Table 8

A key feature shown in Table 8 is that AM1 is remarkably accurate for both the alkyl-alkane reactions and the broader BH6 test set. The effort of adding one parametrized Gaussian in AM1-CHC-SRP only slightly improves the barrier heights for alkyl-alkane reactions. The SAM1 method, which is supposed to be a direct improvement on AM1, is not an improvement for barrier heights. PM3 is more accurate than SAM1, but less accurate than AM1, and all attempts to fix it (both new attempts in the present paper, like PM3-3H2, PM3-CHC-SRP, PM3-AHR, and PM3-NHR, and also attempts already available in the literature, like PM3tm, PDDG/PM3, and PM5) make it worse for the BH6 test set, although PM3-CHC-SRP, PM3-NHR, and PM3tm are more accurate for the narrower alkyl-alkane test set. The fact that PM3-CHC-SRP does not systematically improve PM3 indicates that probably the success of PM3tm for alkyl-alkane reactions is fortuitous. The recent MSINDO method has never previously been systematically

tested for barrier heights, and the present tests show that is not very accurate for barrier heights, although Table 1 shows that it does remarkably well for the atomization energies.

3-2. Geometries. Tables 9 and 10 list breaking and forming bond lengths and the bond angles at the transferred hydrogen calculated for the transition states. Analysis of these geometrical parameters shows that in case of the $CH_3^\bullet + CH_4$ reaction the distance between transferred hydrogen atom and its donor and acceptor is 1.335 – 1.345 Å, and these three atoms are collinear. The $C_2H_5^\bullet + C_2H_6$ reaction presents a slightly more complicated case where parameters other than interatomic distances also determine the geometry of the system; in this reaction the breaking and forming C-H bonds are slightly elongated (1.340 – 1.350 Å) compared to the $CH_3^\bullet + CH_4$ system. For $C_3H_7^\bullet + C_3H_8$, the MP2 values of the C–H distances are shorter by about 0.02 Å. Among NDO methods, the AM1 and PM3tm methods again performed the best although they underestimate C-H bonds by about 0.05 Å, while other PMx methods give much worse results, e.g., PM5 underestimates the breaking C-H distance by 0.1 Å!

Table 9 and 10

One striking feature of the PM3tm results obtained with SPARTAN deserve special attention, namely that it predicts unsymmetrical saddle points for the critical C-H bonds. Moreover we have noticed that asymmetry is also pronounced in other geometrical parameters (such as bond angles and C-C distances) resulting from PM3tm calculations. This is shown in Figure 1 and Table 11 for the $C_2H_5^\bullet + C_2H_6$ system. It is certainly possible for a symmetric potential energy surface to have asymmetric twin saddle points with a well between them. However, we did a potential energy surface (PES) survey for the $CH_3^\bullet + CH_4$ reaction by PM3tm partial geometry optimizations with C–H distances (carbons to the transferred hydrogen) constrained to values

between 1.22 and 1.38 Å. The results are plotted in Figure 2, which shows that the potential energy contours of this reduced dimensional PES display unsymmetrical features, and disproves the existence of the twin saddle points. To elucidate the source of this asymmetry in PM3tm transition states, we compared PM3tm with two of our methods that are most close to it, namely PM3-AHR and PM3-NHR. We found that the PM3-NHR method also predict asymmetric transition states (as shown in Table 9), which reproduces the PM3tm results to a large extent, while the PM3-AHR method does not give any observable asymmetry in the optimized transition states. The only difference between PM3-AHR and PM3-NHR is that the former includes all hydrogen pairs in the HH repulsive Gaussian, and the latter only includes the nonbonded ones. Specifically, in the PM3-NHR method, we assume that the closest neighbor of a given hydrogen is the atom bonded to it. This assumption is quite appropriate for a stable species because hydrogen can only bond to one atom. However, this definition of bonding can be ambiguous for transition state species, especially the transition state in hydrogen atom transfer reactions, where the transferred hydrogen is half bonded to both of the hydrogen donor and acceptor, and one may get unphysical results for a transition state. For example, in the reactions with a hydrogen atom being transferred between two identical carbon centers (denoted A and B), only one carbon center (A) will be considered to bond to the transferred hydrogen in the PM3-NHR method. As a result, the repulsion between a hydrogen on A (HA) and the transferred H will be excluded as a 1-3 bonded pair in the HH Gaussian term. However, the repulsion between a hydrogen on B (HB) and the transferred hydrogen H will be included in the HH Gaussian term, because they are neither 1-2 nor 1-3 bonded hydrogens. Under this circumstance, an artificial asymmetric transition state is expected because the nonbonded hydrogen repulsions are included unsymmetrically for a species that should be symmetric.

Table 11

Figure 1 and 2

In order to evaluate the geometrical predictions more systematically, we calculated consensus values for the geometrical parameters of the saddle points by averaging the first five available values in each column of Tables 9 and 10. Thus, for example, for $CH_3–H–CH_3$ we used an average of MCG3/3, MC-QCISD/3, SAC-3, QCISD/6-311G(d,p), and MPW1K/MG3S, whereas for $C_3H_7–H–C_3H_7$ (*gauche*), we used an average of SAC-3, MPW1K/6-31+G(d,p), MPW1K/MIDIY+, MPW1K/6-31G(d), and B3LYP/6-31G(2df,p). The resulting consensus values are shown in Table 12, and the mean signed and unsigned errors are in Table 13. In preparing Table 13, in the symmetric cases where PM3tm has an unsymmetrical structure, we compare the average of the forming and breaking bond lengths to the consensus values; the error for this method would be larger if we used the actual bond lengths in the unsymmetrical structures. The two SRP methods give most accurate results, satisfying our goal of parametrization. The AM1-CHC-SRP and PM3-CHC-SRP models agree with the consensus C–H bond distances with MUEs of 0.020 Å and 0.010 Å respectively. Using the parametrized Gaussian for AM1, the large errors for bond angles are also greatly reduced from 1.7 degrees (AM1) to 0.9 degrees (AM1-CHC-SRP). Table 13 also shows that PM3, PM3-3H2, PM3tm, and PM3-NHR give the reasonably accurate transition state geometries (if we ignore the problem with PM3tm and PM3-NHR transition states being unsymmetrical), with AM1 only slightly worse. Note that PM3, PM3-3H2, and AM1 all slightly underestimate the C–H bond distances, and SAM1, MSINDO, MNDO, MNDOC, and PM5 all seriously underestimate the C–H bond distances, whereas adding too much HH repulsion tends to increase these distances. Therefore PM3-AHR overestimates these distances. The improvement in C–H bond distances exhibited by

PM3-CHC-SRP as compared to PM3-AHR is particularly notable, and it may be directly attributed to including bond distances in eq. (3).

Tables 12 and 13

Next we register some of our concerns regarding the SRP models, i.e., AM1-CHC-SRP and PM3-CHC-SRP. It is impressive that these SRP methods give accurate barrier heights (with MUE ~ 1 kcal/mol) and simultaneously predict accurate transition state geometries for alkyl-alkane reactions. However, it is worthwhile to note that the overall performance over the BH6 representative data set becomes worse. This is mainly due to the fact that AM1 and PM3 both give positive mean signed errors (MSEs) on BH6 (see supporting information). In particular, AM1 generally overestimates barrier heights to a greater extent than PM3. Nevertheless, both AM1 and PM3 underestimate the barrier heights for CHC reactions. Therefore, SRPs are necessary for AM1 and PM3 to increase the barrier heights for this specific type of reactions, but the overall performance is sacrificed. Following the same reasoning, these SRP models will not necessarily give good geometries in a global sense, because they are only parametrized against transition state geometries for CHC reactions. Finally we comment that adding Gaussian repulsions is probably not, in general, the best way to reparametrize NDO methods; in fact the present paper would probably lead one to that conclusion if one did not already believe this. The sole reason for using Gaussian repulsions in the present study is to systematically follow up on the observed empirical success of PM3tm for CHC reactions. In the process we did develop useful SRP models for CHC reactions, but a better strategy in the long run is probably to instead (or also) optimize the resonance integrals in the NDO Fock operators.

To study the systematic errors that SRP methods may introduce into geometries of species other than a transition state, we evaluate the differences in C–H bond distance between transition states and the reactants in CHC reactions. These differences of bond distances obtained by AM1,

PM3, AM1-CHC-SRP, and PM3-CHC-SRP are compared to consensus values in Table 14, where the consensus data are obtained in the same way as Table 12. Table 14 shows that both AM1 and PM3 underestimate the difference of C–H distances between transition states and reactants. It is encouraging that both SRP methods, especially the PM3-CHC-SRP method, improve these differences and agree with consensus values better. Thus, the SRP methods we proposed in the present paper for CHC reactions actually reduce the systematic errors in terms of the geometric difference between the transition state and reactants.

Table 14

A sensitive check of whether the improvement in the quality of the SRP surfaces for energies and geometries might have caused other features of the surface to be inaccurate is provided by vibrational frequencies. As mentioned in the Introduction, vibrational frequencies are very important for calculating kinetic isotope effects; they are also important for calculations of absolute reaction rates. In Table 15, we give the frequencies obtained by AM1, PM3, AM1-CHC-SRP, and PM3-CHC-SRP for CH_4. We found that frequencies calculated on SRP surfaces deviate from the original AM1 and PM3 frequencies by only a small amount, which is gratifying. The ratios of SRP frequencies to those calculated by the standard methods are $0.99 - 1.00$ and $0.92 - 0.97$ for AM1-CHC-SRP and PM3-CHC-SRP respectively, whereas the recommended frequency scaling factors (for fundamental frequencies) for AM1 and PM3 are 0.9532 and 0.9761.[65] Table 15 show that, as compared to experiment,[66] three of the four frequencies on the AM1-CHC-SRP surface become more accurate than AM1, whereas for PM3-CHC-SRP, two become more accurate, and two become less accurate than PM3.

Table 15

4. Software

A new version of the MOPAC computer program is now available.[67] This program allows one to carry out PM3-AHR, AM1-SRP, and PM3-SRP calculations in which one or two Gaussian of the form of eq. (2) are added for all hydrogen repulsions. Energies, gradients, and Hessians are all included for the new options. We did not include the NHR option in the code because that is a flawed method in that it does not have continuous gradients, and it does not have the correct symmetry properties.

5. Concluding remarks

In this contribution we have provided benchmark calculations for the geometries and barrier heights of the transition states for the transfer of hydrogen atoms between carbon centers. The we use these results as well as broader test suites of barrier heights and atomization energies (the atomization energies is the sum of the bond energies for successively breaking all the bonds in a molecule) to compare the performance of various semiempirical molecular orbital theories of the NDDO and INDO types, in particular 9 previous and 5 new NDDO methods and one recent INDO method. For hydrogen atom transfer between carbon centers, we find that one of the standard semiempirical NDDO methods, namely AM1, and two new NDDO methods, namely, PM3-CHC-SRP and AM1-CHC-SRP, provide reasonable energies and geometrical parameters in comparison to those obtained at high levels of theory. The other ten standard models and the other three new models all have large average errors (> 5 kcal/mol) in barrier heights or give unphysical asymmetric saddle point geometries. To test the generality of this finding and to provide a validation suite that will be useful in a wider context, all 16 NDDO and INDO methods are tested against more broadly representative benchmarks for both atomization energies and barrier heights. The most accurate methods in these broader tests are (in order of decreasing

accuracy) the new PM3-H2 method, the original PM3 method, the new symmetry-deficient PM3-NHR method, and the AM1 method.

References

(1) (a) Fersht, A. *Enzyme Strucutre and Mechanism,* 2nd ed., W.H. Freeman: New York, 1985. (b) Kreevoy, M. M.; Truhlar, D. G. In *Investigation of Rates and Mechanisms of Reactions*; Bernasconi, C. F., Ed.; Techniques of Chemistry Series, Vol. b; Wiley: New-York, 1986; Part I, pp. 13-95. (c) Truhlar, D. G.; Garrett, B. C.; Klippenstein, S. J. *J. Phys. Chem.* **1996**, *100*, 12771.

(2) Gao, J.; Truhlar, D. G. *Annu. Rev. Phys. Chem.* **2002**, *53*, 467.

(3) (a) Brooks, H. B.; Jones, L. H.; Davidson, V. L. *Biochemistry* **1993**, *32*, 2725. (b) Bahnson, B. J.; Klinman, J. P. *Methods Enzymol.* **1995**, *249*, 373. (c) Glickman, M. H.; Klinman, J. P. *Biochemistry* **1995**, *34*, 14077. (d) Glickman, M. H.; Klinman, J. P. *Biochemistry* **1996**, *35*, 12882. (e) Marsh, E. N. G.; Ballou, D. P. *Biochemistry* **1998**, *37*, 11864. (f) Alhambra, C.; Gao, J.; Corchado, J. C.; Villa, J.; Truhlar, D. G. *J. Am. Chem. Soc.* **1999**, *121*, 2253. (g) Bahnson, B. J.; Park, D.-H.; Plapp, B. V.; Klinman, J. P. *Biochemistry* **1999**, *32*, 5503. (h) Basran, J.; Sutcliffe, M. J.; Scrutton, N. S. *Biochemistry* **1999**, *38*, 3218. (i) Alhambra, C.; Gao, J.; Corchado, J. C.; Sanchez, M. L.; Truhlar, D. G. *J. Am. Chem. Soc.* **2000**, *122*, 8197. (j) Billeter, S. R.; Webb, S. P.; Iordanov, T.; Agarwal, P. K.; Hammes-Schiffer, S. *J. Am. Chem. Soc.* **2001**, *123*, 6925. (k) Villa, J.; Warshel, A. *J. Phys. Chem. B* **2001**, *105*, 7887. (l) Garcia-Viloca, M.; Alhambra, C.; Truhlar, D. G.; Gao, J. *J. Comp. Chem.* **2002**, *24*, 177.

(4) (a) Padmakumar, R.; Padmakumar, R.; Banerjee, R. *Biochemistry* **1997**, *36*, 3713. (b) Chowdhury, S.; Banerjee, R. *J. Am. Chem. Soc.* **2000**, *122*, 5417.

(5) (a) Becke, A. D., *J. Chem. Phys.* **1993**, *98*, 5648. (b) Truong, T. N.; Duncan, W. T.; Bell, R. L. *ACS Symp. Ser.* **1996**, *629*, 85. (c) Stephens, P. J.; Devlin, F. J.; Ashvar, C. S.; Bak, K. L.; Talyor, P. R.; Frisch, M. J. *ACS Symp. Ser.* **1996**, *629*, 105. (d) Baker, J.; Muir, M.; Andzelm, J.; Scheiner, A. *ACS Symp. Ser.* **1996**, *629*, 342.

(6)   Lynch, B. J., Fast, P. L., Harris, M., Truhlar, D. G. *J. Phys. Chem. A* **2000**, *104*, 4811.

(7)   (a) Dewar, M. J. S.; Zoebisch, E. G.; Healy, E. F.; Stewart, J. J. P. *J. Am. Chem. Soc.* **1985**, *107*, 3902. (b) Holder, A. J.; Dennington, R. D.; Jie, C.; Yu, G. *Tetrahedron*, **1994**, *50*, 627. (c) Dewar, M. J. S.; Jie, C.; Yu, G. *Tetrahedron*, **1993**, *23*, 5003.

(8)   Stewart, J. J. P. *J. Comp. Chem.* **1989**, *10*, 209.

(9)   (a) Kawamura, H.; Kumar, V.; Sun, Q.; Kawazoe, Y. *Phys. Rev. B* **2001**, *65*, 045406/1. (b) Oefner, H.; Zaera, F. *J. Am. Chem. Soc.* **2002**, *124*, 10982. (c) Wright, S.; Skelly, J. F.; Hodgson, A. *Chem. Phys. Lett.* **2002**, *264*, 522. (d) Bukoski, A.; Harrison, I. *J. Chem. Phys.* **2003**, *118*, 9762.

(10)   (a) Mancia, F.; Evans, P. R. *Structure* (London) **1998**, *6*, 711. (b) Chowdhury, S.; Banerjee, R. *Biochemistry* **2000**, *39*, 7998. (c) Dybala-Defratyka, A.; Paneth, P. *J. Inorg. Biochemistry*, **2001**, *86*, 681.

(11)   Zerner, M. C. *Rev. Comp. Chem.* **1991**, *2*, 313.

(12)   (a) Roothaan, C. C. J. *Rev. Mod. Phys.* **1951**, *23*, 69. (b) Pople, J. A.; Nesbet, R. K. *J. Chem. Phys.* **1954**, *22*, 571.

(13)   (a) Møller, C.; Plesset, M. S. *Phys. Rev.* **1934**, *46*, 618. (b) Pople, J. A.; Binkley, J.; Seeger, R. *Int. J. Quantum Chem. Symp.* **1976**, *10*, 1.

(14)   (a) Tratz, C. M.; Fast, P. L.; Truhlar, D. G. *PhysChemComm* **1999**, *2*, Article 14. (b) Fast, P. L.; Sanchez, M. L.; Truhlar, D. G. *Chem. Phys. Lett.* **1999**, *306*, 407.

(15)   Lynch, B. J.; Truhlar, D. G. *J. Phys. Chem. A* **2003**, *107*, 3898.

(16)   Fast, P. L.; Truhlar, D. G. *J. Phys. Chem. A*. **2000**, *104*, 6111.

(17)   Gordon, M. S.; Truhlar, D. G. *J. Am. Chem. Soc.* **1986**, *108*, 5412.

(18)   Curtiss, L. A.; Redfern, P. C.; Raghavachari, K.; Rassolov, V.; Pople, J. A. *J. Chem. Phys.* **1999**, *110*, 4703.

(19)   Curtiss, L. A.; Redfern, P. C.; Raghavachari, K.; Pople, J. A. *J. Chem. Phys.* **2001**, *114*, 108.

(20)   Petersson, G. A.; Al-Laham, M. A. *J. Chem. Phys.* **1991**, *94*, 6081.

(21)   Ochterski, J. W.; Petersson, G. A.; Montgomery Jr., J. A. *J. Chem. Phys.* **1996**, *104*, 2598.

(22)   (a) Montgomery Jr., J. A.; Frisch, M. J.; Ochterski, J. W.; Petersson, G. A. *J. Chem. Phys.* **1999**, *110*, 2822. (b) Montgomery Jr., J. A.; Frisch, M. J.; Ochterski, J. W.; Petersson, G. A. *J. Chem. Phys.* **2000**, *112*, 6532.

(23)   Binkley, J. S.; Pople, J. A.; Hehre, W. J. *J. Am. Chem. Soc.* **1980**, *102*, 939.

(24)   (a) Hariharan, P. C.; Pople, J. A. *Theor. Chim. Acta* **1973**, *28*, 213. (b) Francl, M. M.; Pietro, W. J.; Hehre, W. J.; Binkley, J. S.; Gordon, M. S.; DeFrees, D. J.; Pople, J. A. *J. Chem. Phys.* **1982**, *77*, 3654.

(25)   Curtiss, L. A.; Raghavachari, K.; Redfern, P. C.; Rassolov, V.; Pople, J. A. *J. Chem. Phys.* **1998**, *109*, 7764.

(26)   Lynch, B. J.; Truhlar, D. G. *J. Phys. Chem.* **2001**, *105*, 2936.

(27)   Lynch, B. J.; Truhlar, D. G. *Theor. Chem. Acc.*, in press.

(28)   Easton, R. E.; Giesen, D. J.; Welch, A.; Cramer, C. J.; Truhlar, D. G. *Theor. Chim. Acta.* **1996**, *93*, 281.

(29)   (a) Lynch, B. J.; Zhao, Y.; Truhlar, D. G. *J. Phys. Chem. A* **2003**, *107*, 1384. (b) Krishnan, R.; Binkley, J. S.; Seeger, R.; Pople, J. A. *J. Chem. Phys.* **1980**, *72*, 650.

(30) Frisch, M. J.; Trucks, G. W.; Schlegel, H. B.; Scuseria, G. E.; Robb, M. A.; Cheeseman, J. R.; Zakrzewski, V. G.; Montgomery Jr., J. A.; Stratmann, R. E.; Burant, J. C.;

Dapprich, S.; Millam, J. M.; Daniels, A. D.; Kudin, K. N.; Strain, M. C.; Farkas, O.; Tomasi, J.; Barone, V.; Cossi, M.; Cammi, R.; Mennucci, B.; Pomelli, C.; Adamo, C.; Clifford, S.; Ochterski, J.; Petersson, G. A.; Ayala, P. Y.; Cui, Q.; Morokuma, K.; Malick, D. K.; Rabuck, A. D.; Raghavachari, K.; Foresman, J. B.; Cioslowski, J.; Ortiz, J. V.; Stefanov, B. B.; Liu, G.; Liashenko, A.; Piskorz, P.; Komaromi, I.; Gomperts, R.; Martin, R. L.; Fox, D. J.; Keith, T.; Al-Laham, M. A.; Peng, C. Y.; Nanayakkara, A.; Gonzalez, C.; Challacombe, M.; Gill, P. M. W.; Johnson, B.; Chen, W.; Wong, M. W.; Andres, J. L.; Head-Gordon, M.; Replogle, E. S.; Pople, J. A. *Gaussian 98*, A.11.

(31) (a) Rodgers, J. M.; Lynch, B. J.; Fast, P. L.; Chuang, Y.-Y.; Pu, J.; Truhlar, D. G. MULTILEVEL-version 2.4/G98; University of Minnesota, Minneapolis, 2001. (b) Rodgers, J. M.; Lynch, B. J.; Fast, P. L.; Chuang, Y.-Y.; Pu, J.; Zhao, Y.; Truhlar, D. G. MULTILEVEL-version 3.0.1/G98; University of Minnesota, Minneapolis, 2002.

(32) Fast, P.L.; Corchado, J.; Sanchez, M. L.; Truhlar, D. G. *J. Chem. Phys. A* **1999**, *103*, 3139.

(33) Stewart, J. J. P., Rossi, I., Hu, W.-P., Lynch, G. C., Liu, Y.-P., Chuang, Y.-Y., Li, J., Cramer, C. J., Fast, P. L., Truhlar, D. G., MOPAC-version 5.09mn, University of Minnesota, Minneapolis, 1999.

(34) (a) SPARTAN PRO version 1.0.5, Wavefunction, Inc., Irvine, CA, U.S.A. (b) SPARTAN '02WIN,Wavefunction, Inc., Irvine, CA, U.S.A.

(35) Stewart, J. J. P. MOPAC2002, Fujitsu Limited, Tokyo, Japan.

(36) Stewart, J. J. P. MOPAC v2.2, FQS, Poland, 2002.

(37) (a) Dewar, M. J. S.; Jie, C.; Yu, G. *Tetrahedron* **1993**, *23*, 5003. (b) Holder, A. J.; Dennington, R. D.; Jie, C.; Yu, G. *Tetrahedron* **1994**, *50*, 627.

(38) (a) Dewar, M. J. S.; Thiel, W. *J. Am. Chem. Soc.* **1997**, *99*, 4499. (b) Dewar, M. J. S.; Thiel, W. *J. Am. Chem. Soc.* **1977**, *99*, 4899.

(39) (a) Thiel, W.; Voityuk, A. A. *Theor. Chim. Acta.* **1992**, *81*, 391. (b) Thiel, W.; Voityuk, A. A. *Theor. Chim. Acta.* **1996**, *93*, 315. (b) Thiel, W.; Voityuk, A. A. *Intern. J. Quant. Chem.* **1992**, *44*, 807. (c) Thiel, W.; Voityuk, A. A. *J. Mol. Struct.* **1994,** *313*, 141.

(40) Thiel, W. *J. Am. Chem. Soc.* **1981**, *103*, 1413.

(41) AMPAC 7.0, Semichem, Inc., P.O. Box 1649, Shawnee Mission, KS 66222-0649.

(42) Ahlswede, B.; Jug, K. *J. Comp. Chem.* **1999**, *20*, 563.

(43) Jug, K.; Bredow, T.; Geudtner, G. MSINDO-version 2.6, University of Hannover, Hannover, Germany, 2003.

(44) Repasky, M. P.; Chandrasekhar, J.; Jorgensen, W. L. *J. Comp. Chem.* **2002**, *23*, 1601.

(45) See: http://zarbi.chem.yale.edu/utils/pddg/pddg.html

(46) Pople, J. A.; Santry, D. P.; Segal, G. A. *J. Chem. Phys.* **1965**, *43*, S129.

(47) Pople, J. A.; Beveridge, D. L.; Dobosh, P. A. *J. Chem. Phys.* **1967**, *47*, 2026.

(48) Lynch B. J.; Truhlar, D. G. *J. Phys. Chem. A*, in press.

(49) Raghavachari, K.; Anderson, J. B. *J. Phys. Chem.* **1996**, *100*, 12960.

(50) Kerr, J. A.; Moss, S. J. *CRC Handbook of Bimolecular and Termolecular Gas Reactions*, Vol.1 CRC Press, Boca Raton, 1981.

(51) Marcus, R. A. *Annu. Rev. Phys. Chem.* **1964**, *15*, 155.

(52) Marcus, R. A. *J. Phys. Chem.* **1968**, *72*, 891.

(53) Cohen, A. O.; Marcus, R. A. *J. Phys. Chem.* **1968**, *72*, 4249.

(54) Wolfe, S.; Mitchell, D. J.; Schlegel, H. B. *J. Am. Chem. Soc.* **1981**, *103*, 7694.

(55) Kreevoy, M. M.; Truhlar, D. G. In *Investigations of Rates and Mechanisms of Reactions*; Bernasconi, C. F., Ed.; Techniques of Chemistry Series 6/1; Wiley: New York, 1986; p. 13.

(56) Wladkowsky, B. D.; Brauman, J. I. *J. Phys. Chem.* **1993**, *97*, 13158.

(57) Guthrie, J. P. *J. Am. Chem. Soc.* **1996**, *118*, 12886.

(58) Roth, J. P.; Yoder, J. C.; Won, T.-J.; Mayer, J. M. *Science* **2001**, *294*, 2524.

(59) (a) Litwinowicz, J. A.; Ewing, D. W.; Jurisevic, S.; Manka, M. J. *J. Phys. Chem.* **1995**, *99*, 9709. (b) Jursic, B. S. *Chem. Phys. Lett*. **1995**, *244*, 263.

(60) (a) Csonka, G. I. *J. Comp. Chem.* **1993**, *14*, 895. (b) Csonka, G. I.; Angyan, J. G. *J. Mol. Struct. (Theochem)* **1997**, *393*, 31.

(61) (a) Bernal-Uruchurtu, M. I.; Ruiz-Lopez, M. F. *Chem. Phys. Lett.* **2000**, *330*, 118. (b) Bernal-Uruchurtu, M. I.; Martins-Costa, M. T. C.; Millot, C.; Ruiz-Lopez, M. F. *J. Comp. Chem.* **2000**, *21*, 572.

(62) http://www.organic.gu.se/dissertation/Sten_diss.pdf

(63) Carroll, D. L. *FORTRAN Genetic Algorithm (GA) Driver*. See: http://cuaerospace.com/carroll/ga.html

(64) Gonzalez-Lafont, A.; Truong, T. N.; Truhlar, D. G. *J. Phys. Chem.* **1991**, *95*, 4618.

(65) Scott, A. P.; Radom, L. *J. Phys. Chem.* **1996**, *100*, 16502.

(66) Herzberg, G. *Molecular Spectra and Molecular Structure III. Electronic Spectra and Electronic Structure of Polyatomic Molecules*; Van Nostrand Reinhold: New York, 1966; p. 619.

(67) Stewart, J. J. P.; Rossi, I.; Hu, W.-P.; Lynch, G. C.; Liu, Y.-P.; Chuang, Y.-Y.; Pu, J.; Li, J.; Cramer, C. J.; Fast, P. L.; Truhlar, D. G. MOPAC-version 5.10mn, University of Minnesota, Minneapolis, 2003.

TABLE 1. Mean Unsigned Error (MUE in kcal/mol) for Methods Over the Representative Data Set[a]

Method	BH6	BH4	AE6[b]	AE3[b]
N[7]				
G3S//MP2(full)/6-31G(d)[c]	0.37	0.46	0.20	0.16
G3SX(MP3)//B3LYP/6-31G(2df,p)	0.39	0.38	0.15	0.11
CBS-APNO//QCISD/6-311G(d,p)	n.a.[d]	1.21	n.a.	0.16
CBS-QB3//B3LYP/6-31G(d†)	0.68	0.84	0.34	0.20
MCG3/3	n.c.[e]	n.c.	n.c.	n.c.
MCG3/3//MPW1K/6-31+G(d,p)	0.76	0.53	0.22	0.07
CBS-Q//MP2/6-31G(d†)	0.81	1.01	0.34	0.20
N[6]				
MC-QCISD/3//MPW1K/6-31+G(d,p)	0.72	0.59	0.19	0.08
MC-QCISD/3	0.87	0.76	n.c.	n.c.
CBS-4M//UHF/3-21G(d)	2.30	3.19	0.53	0.34
N[5]				
SAC/3	3.08	3.60	1.51	0.73
MP2/6-31+G(d,p)	5.60	5.80	4.85	4.09
MP2/6-31G(d)	7.00	6.98	6.36	6.74
N[4]				
MPW1K/MG3S	1.41	1.49	2.08	1.54
MPW1K/6-31+G(d,p)	1.41	1.77	2.95	1.89
MPW1K/MG3S//MPW1K/6-31+G(d,p)	1.42	1.51	2.11	1.56
MPW1K/MIDIY+	2.03	2.21	5.03	4.94
MPW1K/6-31G(d)	2.67	3.80	2.98	1.79
B3LYP/6-31+G(d,p)	5.11	6.43	1.39	0.90
HF/MIDI!	11.03	12.72	34.71	34.55
HF/6-31+G(d,p)	13.40	14.99	30.74	29.33
HF/6-31G(d)	13.73	15.25	31.04	29.48
N[3]				
PM3-3H2[f]	3.01	2.99	3.32	3.16
AM1	4.40	5.28	5.38	3.67
PM3	4.96	4.13	3.32	3.16
AM1-CHC-SRP[f]	5.22	6.38	5.81	4.11
PM3-NHR[f]	6.06	5.79	3.32	3.16
PM3-AHR[f]	7.14	6.91	4.10	4.14
PM3-CHC-SRP[f]	7.42	7.17	4.26	4.24
PM3tm	7.68	8.21	4.35	3.16
SAM1	9.47	5.56	6.20	2.27
MSINDO	10.42	9.33	0.68	0.62
PM5	11.35	5.56	3.87	3.20

MNDO	17.83	24.81	2.76	2.99
MNDO/d	20.44	24.81	5.98	2.99
PDDG/PM3	n.a.	7.56	n.a.	2.76
PDDG/MNDO	n.a.	23.79	n.a.	13.22
MNDOC	n.a.	24.41	n.a.	0.58

[a]See Ref. 48 and http://comp.chem.umn.edu/database/
[b]in kcal/mol per bond (counting double bonds and triple bonds as a single bond).
 Molecules in AE6 and AE3 contain 29 and 23 bonds respectively.
[c]X//Y denotes a single-point calculation by method X at geometry optimized by
 method Y. When no // is present, X and Y are the same.
[d]n.a. denotes that the method is not available for second row elements.
[e]n.c. denotes not calculated.
[f]new method in this article

TABLE 2. Classical Barrier Heights (in kcal/mol) for C_nH_{2n+1}• + C_nH_{2n+2} Hydrogen Atom Transfer Reactions

Method	$n=1$	$n=2$ (g^a)	$n=2$ (t^b)	$n=3$ (g)	$n=3$ (t)
N^7					
G3S//MP2(full)/6-31G(d)	**17.81**	16.33	**16.33**	n.c.	n.c.
G3SX(MP3)//B3LYP/6-31G(2df,p)	17.74	16.52	16.55	**15.90**	15.97
CBS-APNO//QCISD/6-311G(d,p)	**16.66**	n.c.^{c}	n.c.	n.c.	n.c.
CBS-QB3//B3LYP/6-31G(d†)	17.36	16.11	**16.10**	n.c.	n.c.
MCG3/3	**17.90**	n.c.	n.c.	n.c.	n.c.
MCG3/3//MPW1K/6-31+G(d,p)	17.93	**16.52**	16.59	**15.93**	15.99
CBS-Q//MP2/6-31G(d†)	17.34	15.82	15.85	14.76	**14.60**
N^6					
MC-QCISD/3//MPW1K/6-31+G(d,p)	17.96	16.82	16.89	**16.34**	16.41
MC-QCISD/3	**17.95**	**16.74**	16.83	n.c.	n.c.
CBS-4M//UHF/3-21G(d)	17.23	15.59	15.62	15.06	15.13
N^5					
SAC/3	18.27	16.11	16.17	15.25	15.38
MP2/6-31+G(d,p)	21.27	19.39	19.41	18.57	18.68
MP2/6-31G(d)	22.13	20.28	20.31	19.51	19.57
N^4					
MPW1K/MG3S	**17.31**	17.65	**17.57**	n.c.	n.c.
MPW1K/6-31+G(d,p)	16.85	17.12	17.06	17.01	16.98
MPW1K/MG3S//MPW1K/6-31+G(d,p)	17.30	17.72	17.63	17.48	**17.41**
MPW1K/MIDIY+	16.54	16.28	16.18	16.01	15.92
MPW1K/6-31G(d)	16.58	16.76	16.72	16.60	16.57
B3LYP/6-31+G(d,p)	15.00	15.80	15.68	x^d	15.52
HF/MIDI!	28.57	28.42	28.38	28.41	28.38
HF/6-31+G(d,p)	30.47	30.60	30.56	30.59	30.57
HF/6-31G(d)	30.17	30.33	30.28	30.32	30.27
N^3					
PM3-3H2	10.14	12.03	12.06	11.38	11.41
AM1	13.49	16.02	16.05	15.56	15.59
PM3	10.14	11.99	12.06	12.47	12.61
AM1-CHC-SRP	16.11	18.28	18.28	17.88	17.89
PM3-NHR	16.54	16.25	16.26	15.57	15.58
PM3-AHR	13.13	13.90	13.94	13.02	13.22
PM3-CHC-SRP	17.40	17.00	17.01	16.31	16.33
PM3tm	16.66	16.23	16.30	15.48	15.62
SAM1	3.90	7.16	7.14	6.84	6.82
MSINDO	27.38	31.19	31.14	31.29	31.25
PM5	5.91	x	8.71	7.95	7.96

MNDO, MNDO/d[e]	28.59	32.15	32.12	32.45	32.41
PDDG/PM3	6.51	8.29	8.30	7.33	7.36
PDDG/MNDO	20.36	23.41	23.73	22.80	22.08
MNDOC	21.20	25.54	25.52	25.75	25.73

[a]*g* denotes the *gauche* conformation.

[b]*t* denotes the *trans* conformation.

[c]n.c. denotes not calculated.

[d]cannot be optimized to the specified conformation

[e]MNDO and MNDO/d are the same for reactions in this table.

TABLE 3. Classical Barrier Heights and Reaction Energy (in kcal/mol) for $CH_3^\bullet + C_2H_6$.

Method	$V_f{}^a$	$V_r{}^b$	ΔE
N^7			
G3S//MP2(full)/6-31(d)	15.41	18.79	-3.37
G3SX(MP3)//B3LYP/6-31G(2df,p)	**15.39**	**18.85**	-3.45
CBS-APNO//QCISD/6-311G(d,p)	n.c.^{c}	n.c.	-3.78
CBS-QB3//B3LYP/6-31G(d†)	**14.89**	**18.55**	-3.65
MCG3/3	n.c.	n.c.	-3.36
MCG3/3//MPW1K/6-31+G(d,p)	**15.55**	**18.92**	-3.37
CBS-Q//MP2/6-31G(d†)	14.82	18.45	-3.63
N^6			
MC-QCISD/3//MPW1K/6-31+G(d,p)	15.64	19.14	-3.50
MC-QCISD/3	**15.61**	**19.09**	-3.49
CBS-4M//UHF/3-21G(d)	14.51	18.27	-3.77
N^5			
SAC/3	15.68	18.64	-2.96
MP2/6-31G(d)	19.78	22.70	-2.92
MP2/6-31+G(d,p)	19.01	21.60	-2.59
N^4			
MPW1K/MG3S	**15.32**	**19.52**	-4.20
MPW1K/MG3S//MPW1K/6-31+G(d,p)	15.40	19.61	-4.20
MPW1K/6-31+G(d,p)	14.87	18.97	-4.10
MPW1K/MIDIY+	14.57	18.19	-3.63
MPW1K/6-31G(d)	14.52	18.77	-4.25
B3LYP/6-31+G(d,p)	13.02	17.58	-4.56
HF/MIDI!	27.02	29.89	-2.87
HF/6-31G(d)	28.75	31.62	-2.87
HF/6-31+G(d,p)	29.13	31.77	-2.63
N^3			
PM3-3H2	7.31	15.62	-8.31
AM1	12.01	17.81	-5.80
PM3	7.29	15.60	-8.31
AM1-CHC-SRP	14.54	20.13	-5.61
PM3-NHR	12.11	20.43	-8.32
PM3-AHR	11.55	15.59	-4.04
PM3-CHC-SRP	14.61	20.10	-5.49
PM3tm	12.70	21.02	-8.32
SAM1	0.14	11.76	-11.62
MSINDO	24.70	34.79	-10.09
PM5	4.80	11.16	-6.36
MNDO, MNDO/d^d	79.59	85.89	-6.30

PDDG/PM3	3.45	12.07	-8.62
PDDG/MNDO	18.71	25.17	-6.46
MNDOC	71.81	79.23	-7.42

[a]Forward barrier height

[b]Reverse barrier height

[c]n.c. denotes not calculated.

[d]MNDO and MNDO/d are the same for this reaction.

TABLE 4. Consensus Barrier Heights (in kcal/mol)

Reaction	Consensus barrier height
$CH_3{}^{\bullet} + CH_4$	17.53
$CH_3{}^{\bullet} + C_2H_6$	15.36
$C_2H_5{}^{\bullet} + CH_4$	18.99
$C_2H_5{}^{\bullet} + C_2H_6$	16.69
$C_3H_7{}^{\bullet} + C_3H_8$	16.04

TABLE 5. Optimized HH Repulsive Gaussian Functions in PM3-3H2, PM3-CHC-SRP, and Equivalent Parameters in PM3tm

	A (kcal/mol)	r_0 (Å)	λ (Å)
PM3-3H2	7.476	0.764	0.330
PM3-CHC-SRP	3.198	1.700	0.522
PM3tm[a]	3.459	1.700	0.316
AM1-CHC-SRP	1.064	1.603	0.808

[a]The parameters in this row are also used in PM3-AHR and PM3-NHR.

TABLE 6. Classical Reaction Barrier Heights and Reaction Energies (in kcal/mol) for 23 Reactions Obtained by PM3, PM3-3H2, and PM3-CHC-SRP.

Reactions	PM3			PM3-3H2			PM3-CHC-SRP			Best Estimate		
	V_f^a	V_r^b	ΔE	V_f	V_r	ΔE	V_f	V_r	ΔE	V_f	V_r	ΔE
H + HCl	-6.6	9.4	-16.0	-0.2	8.7	-8.9	-0.1	15.9	-16.0	5.7	8.7	-3.0
OH + H_2	12.2	3.0	9.2	12.5	10.4	2.1	16.6	4.6	12.0	5.7	21.8	-16.1
CH_3 + H_2	18.4	-6.2	24.5	11.4	-6.0	17.4	34.4	-0.1	34.5	12.1	15.3	-3.2
OH + CH_4	10.6	25.9	-15.3	10.6	25.8	-15.3	13.0	35.6	-22.5	6.7	19.6	-12.9
H + CH_3OH	0.2	38.7	-38.6	0.2	31.5	-31.4	-10.6	34.9	-45.5	7.3	13.3	-6.0
H + H_2	-19.7	-19.7	0.0	-0.2	-0.2	0.0	-17.0	-17.0	0.0	9.6	9.6	0.0
OH + NH_3	13.6	31.6	-18.0	13.6	31.6	-18.0	17.0	38.4	-21.3	3.2	12.7	-9.5
CH_3 + HCl	-0.3	-8.8	8.5	-0.3	-8.8	8.5	8.6	-9.9	18.5	1.7	7.9	-6.2
OH + C_2H_6	8.1	31.7	-23.6	8.1	31.7	-23.6	10.7	38.7	-28.0	3.4	19.9	-16.5
F + H_2	-3.8	12.3	16.1	-3.5	19.8	-23.3	-3.8	12.4	-16.2	1.8	33.4	-31.6
O + CH_4	10.8	26.6	15.7	10.8	26.6	-15.7	10.2	36.0	-25.8	13.7	8.1	5.6
H + PH_3	-0.2	36.5	-36.6	-0.2	29.2	-29.5	-1.2	39.5	-40.7	3.1	23.2	-20.1
H + ClH'	-14.3	-14.3	0.0	-14.3	-14.3	0.0	-14.0	-14.0	0.0	18.0	18.0	0.0
H + OH	4.5	13.3	-8.8	12.0	13.6	-1.6	4.7	13.4	-8.7	10.7	13.1	-2.4
H + *trans* N_2H_2	-3.1	53.7	-56.9	-1.2	48.5	-49.7	-1.1	55.7	-56.8	5.9	40.9	-35.0
H + H_2S	-0.1	26.9	-27.0	-1.1	18.8	-19.9	-1.1	28.6	-29.7	3.5	17.3	-13.7
O + HCl	7.1	14.3	-7.3	7.1	14.3	-7.3	7.1	14.3	-7.3	9.8	10.4	-0.6
NH_2 + CH_3	16.9	19.6	-2.8	16.9	19.6	-2.8	25.5	21.4	4.1	8.0	22.4	-14.4
NH_2 + C_2H_5	22.2	16.7	5.5	22.2	16.7	5.5	28.3	18.6	9.6	7.5	18.3	-10.8
C_2H_6 + NH_2	17.2	22.8	-5.6	17.2	22.8	-5.6	22.2	28.9	-6.6	10.4	17.4	-7.0
NH_2 + CH_4	20.4	17.7	2.7	20.4	17.7	2.7	25.0	26.0	-1.1	14.5	17.8	-3.3
s-trans-cis-$C_5H_8^c$	35.6	35.6	0.0	35.6	35.6	0.0	39.0	39.0	0.0	38.4	38.4	0.0
CH_3 + CH_4	10.1	10.1	0.0	10.1	10.1	0.0	17.4	17.4	0.0	17.7	17.7	0.0

[a]Forward barrier height   [b]Reverse barrier height   [c]1,5 sigmatropic shift

TABLE 7. RMSE and MUE (in kcal/mol) for PM3, PM3-3H2, and PM3-CHC-SRP from Best Estimates of Table 5, and Consensus Barrier Heights of Table 3.

Error	PM3	PM3-3H2	PM3-CHC-SRP
RMSE			
ΔE (23 data)	14.9	11.7	18.8
$V^{\ddagger}$ (46 data)	13.6	11.0	15.2
overall (69 data)	14.1	11.3	16.5
consensus barriers (5 data)	5.7	5.9	0.8
MUE			
ΔE (23 data)	11.7	8.9	14.6
$V^{\ddagger}$ (46 data)	12.2	8.2	12.2
overall (69 data)	10.8	8.4	13.0
consensus barriers (5 data)	5.4	5.6	0.7

TABLE 8. Mean Unsigned Errors (in kcal/mol) for Semiemprical Methods

Reaction	vs. Table 4	vs. BH6	vs. BH4
PM3-3H2	5.61	3.01	2.99
AM1	1.93	4.40	5.28
PM3	5.38	4.96	4.13
AM1-CHC-SRP	1.36	5.22	6.38
PM3-NHR	1.33	6.06	5.79
PM3-AHR	3.44	7.14	6.91
PM3-CHC-SRP	0.72	7.42	7.17
PM3tm	1.27	7.68	8.21
SAM1	10.97	9.47	5.56
MSINDO	12.93	10.42	9.33
PM5	9.21	11.35	5.56
MNDO	34.00	19.58	24.81
MNDO/d	34.00	20.44	24.81
PDDG/PM3	9.38	n.a.[a]	7.56
PDDG/MNDO	5.09	n.a.	23.79
MNDOC	27.78	n.a.	24.41

[a]n.a. denotes that the method is not available for second row elements.

TABLE 9. Optimized Transition State Geometries Obtained at Different Levels of Theory for $C_nH_{2n+1}^{\bullet}$ + C_nH_{2n+2} Hydrogen Atom Transfer Reactions[a]

Method	$n=1$		$n=2$ (g[b])			$n=2$ (t[c])			$n=3$ (g)			$n=3$ (t)		
	CH	CHC	CH	CHC	ϕ[d]	CH	CHC	ϕ	CH	CHC	ϕ	CH	CHC	ϕ
MCG3/3	1.342	180.0	n.c.[e]	n.c.	n.c.	n.c.	n.c.	n.c.	n.c.	n.c.	n.c.	n.c.	n.c.	n.c.
MC-QCISD/3	1.339	180.0	1.343	173.5	93.0	1.342	180.0	180.0	n.c.	n.c.	n.c.	n.c.	n.c.	n.c.
SAC-3	1.320	180.0	1.324	174.7	87.8	1.324	180.0	180.0	1.325	175.7	83.7	1.325	180.0	180.0
QCISD/6-311G(d,p)	1.341	180.0	n.c.	n.c.	n.c.	n.c.	n.c.	n.c.	n.c.	n.c.	n.c.	n.c.	n.c.	n.c.
MPW1K/MG3S	1.333	180.0	1.340	177.8	78.3	1.339	180.0	180.0	n.c.	n.c.	n.c.	n.c.	n.c.	n.c.
MPW1K/6-31+G(d,p)	1.334	180.0	1.340	177.8	78.3	1.339	180.0	180.0	1.34	177.8	91.4	1.34	179.6	169.4
MPW1K/MIDIY+	1.331	180.0	1.335	177.6	85.1	1.334	180.0	180.0	1.335	178.0	88.9	1.335	180	180.0
MPW1K/6-31G(d)	1.335	180.0	1.342	178.4	75.2	1.341	180.0	180.0	1.342	178.2	84.2	1.341	179.8	170.7
B3LYP/6-31+G(d,p)	1.347	180.0	1.355	179.0	75.2	1.354	180.0	180.0	x[f]	x	x	1.354	180.0	177.0
B3LYP/6-31G(2df,p)	1.348	180.0	1.356	179.2	69.5	1.355	180.0	180.0	1.355	179.0	73.8	1.355	180.0	176.5
B3LYP/6-31G(d†)	1.347	180.0	1.356	178.8	87.8	1.355	180.0	180.0	n.a.	n.a.	n.a.	n.a.	n.a.	n.a.
MP2/6-31+G(d,p)	1.324	180.0	1.327	176.4	67.6	1.327	177.9	140.0	1.328	175.8	70.5	1.328	180.0	180.0
MP2 (Full) /6-31G(d)	1.331	180.0	1.335	177.5	68.1	1.334	180.0	180.0	1.335	176.8	67.2	1.334	180.0	179.2
MP2/6-31G(d†)	1.333	180.0	1.337	177.0	65.0	1.336	180.0	179.8	1.337	176.6	64.5	1.337	180.0	179.5
MP2/6-31G(d)	1.332	180.0	1.335	177.0	68.1	1.335	180.0	180.0	1.336	176.6	67.3	1.335	180.0	180.0
HF/MIDI!	1.362	180.0	1.362	178.8	86.3	1.362	180.0	180.0	1.362	178.3	84.9	1.362	180	180.0
HF/6-31+G(d,p)	1.356	180.0	1.361	178.6	94.5	1.360	180.0	180.0	1.361	178.7	104.0	1.361	180	179.9
HF/6-31G(d)	1.357	180.0	1.363	178.9	90.4	1.362	180.0	180.0	1.363	178.8	96.1	1.362	179.8	179.9
UHF/3-21G(d)	1.356	180.0	1.356	178.7	81.6	1.355	180.0	180.0	1.357	178.7	81.2	1.357	180.0	180.0
PM3-3H2	1.288	179.8	1.323	179.6	95.4	1.320	179.6	178.1	1.321	176.3	100.8	1.321	178.7	170.5
AM1	1.299	178.9	1.316	173.7	104.4	1.316	179.6	174.2	1.314	174.2	106.4	1.314	179.8	179.3

PM3	1.288	179.8	1.323	176.6	50.1	1.323	179.7	179.4	1.321	175.9	49.5	1.320	179.9	178.9
AM1-CHC-SRP	1.304	179.4	1.322	175.5	107.8	1.322	179.4	179.7	1.320	174.7	105.3	1.320	179.7	168.8
PM3-NHR	1.300 (1.355)	179.3	1.341 (1.360)	176.4	102.2	1.341 (1.362)	177.9	171.4	1.336 (1.360)	180.0	103.0	1.336 (1.360)	180.0	166.4
PM3-AHR	1.376	179.8	1.382	176.9	95.6	1.382	179.7	163.4	1.380	178.7	48.6	1.379	179.	169.5
PM3-CHC-SRP	1.324	179.9	1.351	178.9	98.5	1.351	179.6	158.6	1.348	178.5	104.2	1.349	179.5	170.3
PM3tm	1.303 (1.366)	179.8	1.342 (1.367)	176.9	52.6	1.342 (1.366)	177.9	173.5	1.338 (1.366)	176.9	48.7	1.337 (1.365)	177.9	176.1
SAM1	1.275	179.8	1.303	174.0	91.6	1.300	179.9	179.8	1.300	172.7	81.7	1.303	180.0	179.8
MSINDO	1.268	180.0	1.304	175.6	80.0	1.304	180.0	180.0	1.301	176.3	91.6	1.300	179.7	169.6
PM5	1.249	179.9	x	x	x	1.263	179.6	164.4	1.263	179.7	31.4	1.262	179.5	150.9
MNDO, MNDO/d[g]	1.316	180.0	1.332	176.1	85.4	1.331	180.0	179.4	1.333	180.0	101.1	1.333	180.0	179.8
PDDG/PM3	1.287	179.7	1.317	178.1	107.1	1.317	180.0	177.7	1.314	179.3	104.9	1.315	179.3	164.3
PDDG/MNDO	1.284	179.9	1.309	168.2	112.8	1.310	180.0	179.9	1.308	167.9	119.0	1.308	178.4	169.3
MNDOC	1.291	180.0	1.307	175.6	88.3	1.307	179.9	179.3	1.308	175.2	96.2	1.308	180.0	180.0

[a]Bond lengths are in Å; bond angles and torsions are in degrees.

[b]g denotes the *gauche* conformation.

[c]t denotes the *trans* conformation.

[d]ϕ is the C–C–C–C dihedral angle (for $n = 3$ it corresponds to the four carbons closest to the transferred H).

[e]n.c. denotes not calculated.

[f]cannot be optimized to the specified conformation

[g]MNDO and MNDO/d are the same for reactions in this table.

TABLE 10. Optimized Transition State Geometries Obtained at Different Levels of Theory for the $CH_3^{\bullet}$ + C_2H_6 Hydrogen Atom Transfer Reactions[a]

Method	CH_3–H	H–CH_2CH_3	HCH
MC-QCISD/3	1.365	1.319	176.1
SAC/3	1.344	1.302	176.5
QCISD/6-311G(d,p)	1.362	1.325	177.5
MPW1K/MG3S	1.362	1.312	178.4
MPW1K/6-31+G(d,p)	1.363	1.312	178.4
MPW1K/MIDIY+	1.358	1.310	178.5
MPW1K/6-31G(d)	1.365	1.313	178.5
B3LYP/6-31+G(d,p)	1.380	1.323	179.1
B3LYP/6-31G(2df,p)	1.383	1.322	179.2
B3LYP/6-31G(d[†])	1.381	1.323	178.9
MP2/6-31+G(d,p)	1.343	1.309	177.3
MP2 (Full) /6-31G(d)	1.352	1.315	177.8
MP2/6-31G(d[†])	1.355	1.316	177.6
MP2/6-31G(d)	1.352	1.315	177.8
HF/MIDI!	1.375	1.349	179.0
HF/6-31+G(d,p)	1.370	1.345	178.7
HF/6-31G(d)	1.372	1.346	178.8
UHF/3-21G(d)	1.367	1.343	178.9
PM3-3H2	1.342	1.275	179.0
AM1	1.334	1.284	174.8
PM3	1.343	1.274	179.0
AM1-CHC-SRP	1.339	1.288	177.2
PM3-NHR	1.386	1.287	179.7
PM3-AHR	1.395	1.363	175.6
PM3-CHC-SRP	1.364	1.318	178.6
PM3tm	1.355	1.343	179.3
SAM1	1.357	1.230	174.6
MSINDO	1.326	1.252	176.9
PM5	1.400	1.170	178.6
MNDO, MNDO/d[g]	1.438	1.213	174.9
MNDOC	1.332	1.244	166.9
PDDG/PM3	1.350	1.265	179.7
PDDG/MNDO	1.313	1.277	166.8

[a]Bond lengths are in Å; bond angles and torsions are in degrees.
[g]MNDO and MNDO/d are the same for this reaction.

TABLE 11. Comparison of the Selected Geometrical Parameters of Saddle Point Structure of $C_2H_5^{\bullet} + C_2H_6$ Using the PM3tm (see Figure 1) and MPW1K/6-31+G(d,p) Methods[a]

Parameter	PM3tm	MPW1K/6-31+G(d,p)
5-7	1.367	1.340
5-2	1.342	1.340
7-6	1.483	1.502
2-1	1.492	1.502
7-8	1.089	1.086
7-9	1.089	1.086
2-3	1.102	1.086
2-4	1.102	1.086
5-7-6	109.6	107.7
5-2-1	106.6	107.6

[a]Bond lengths are in Å; bond angles and torsions are in degrees.

TABLE 12. Consensus values for Key Transition State Geometrical Parameters

Parameter	Value
C–H distance (in Å)	
CH_3–H–CH_3	1.335
C_2H_5–H–C_2H_5 (*gauche*)	1.336
C_2H_5–H–C_2H_5 (*trans*)	1.336
C_3H_7–H–C_3H_7 (*gauche*)	1.339
C_3H_7–H–C_3H_7 (*trans*)	1.339
CH_3–H in CH_3–H–C_2H_5	1.359
C_2H_5–H in CH_3–H–C_2H_5	1.314
C–H–C angle (in degrees)	
CH_3–H–CH_3	180.0
C_2H_5–H–C_2H_5 (*gauche*)	176.3
C_2H_5–H–C_2H_5 (*trans*)	180.0
C_3H_7–H–C_3H_7 (*gauche*)	177.7
C_3H_7–H–C_3H_7 (*trans*)	179.9
CH_3–H–C_2H_5	177.4

TABLE 13. Mean Signed and Unsigned Errors in Key Transition State Geometrical Parameters

Method	MSE	MUE
C–H distance[a] (in Å)		
PM3-3H2	-0.033	0.033
AM1	-0.026	0.026
PM3	-0.024	0.024
AM1-CHC-SRP	-0.020	0.020
PM3-NHR	0.012	0.014
PM3-AHR	0.043	0.043
PM3-CHC-SRP	0.007	0.010
PM3tm	-0.004	0.021
SAM1	-0.042	0.042
MSINDO	-0.043	0.043
PM5	-0.069	0.083
MNDO	-0.009	0.031
MNDOC	-0.037	0.037
PDDG/PM3	-0.028	0.028
PDDG/MNDO	-0.036	0.036
C–H–C angle (in degrees)		
PM3-3H2	0.3	1.4
AM1	-1.7	1.7
PM3	0.1	0.9
AM1-CHC-SRP	-0.9	0.9
PM3-NHR	0.3	1.3
PM3-AHR	-0.3	0.8
PM3-CHC-SRP	0.6	0.9
PM3tm	-0.4	1.3
SAM1	-1.7	1.8
MSINDO	-0.5	0.5
PM5	0.5	0.8
MNDO, MNDO/d[b]	-0.1	0.9
MNDOC	-2.3	2.3
PDDG/PM3	0.8	1.1
PDDG/MNDO	-5.0	5.0

[a]All C–H bond distances in tables refer to the forming and breaking bonds.
[b]MNDO and MNDO/d are the same for reactions in this table.

TABLE 14. Difference of C–H Distances in Transition States and Reactants Obtained by AM1, PM3, AM1-CHC-SRP, and PM3-CHC-SRP Compared to Consensus Values[a]

Parameter	AM1	PM3	AM1-CHC-SRP	PM3-CHC-SRP	Consensus
Difference in C–H distance (in Å)					
CH_3–H–CH_3 vs. $CH_3^{\bullet}$	0.213	0.217	0.217	0.244	0.247
CH_3–H–CH_3 vs. CH_4	0.188	0.202	0.192	0.231	0.257
CH_3–H in CH_3–H–C_2H_5 vs. $CH_3^{\bullet}$	0.248	0.271	0.252	0.285	0.282
C_2H_5–H in CH_3–H–C_2H_5 vs. C_2H_6	0.167	0.176	0.168	0.215	0.227
CH_3–H in CH_3–H–C_2H_5 vs. CH_4	0.222	0.256	0.226	0.272	0.272
C_2H_5–H in CH_3–H–C_2H_5 vs. $C_2H_5^{\bullet}$	0.194	0.192	0.196	0.231	0.234

[a]Symmetric H atom transfer reactions $C_nH_{2n+1}^{\bullet} + C_nH_{2n+2}$ ($n = 1, 2, 3$) give similar results for these distances, therefore we only tabulate the $n = 1$ case in this table.

TABLE 15. Vibrational Frequencies of CH_4 Obtained by AM1, PM3, AM1-CHC-SRP, and PM3-CHC-SRP

Frequencies (cm^{-1})	AM1	PM3	AM1-CHC-SRP	PM3-CHC-SRP	experimental[a]
v_1 (a_1)	3216	3313	3184	3094	2917
v_2 (e)	1412	1451	1399	1296	1534
v_3 (t_1)	3104	3268	3083	3106	3019
v_4 (t_2)	1380	1303	1375	1345	1306

[a]Reference 57

Figure Captions

Figure 1.   The optimized saddle point structure of $C_2H_5^{\bullet} + C_2H_6$ using the PM3tm method.

Figure 2.   Potential energy contours (in kcal/mol) for $CH_3^{\bullet} + CH_4$ using the PM3tm method. Geometries are optimized under constraints on the forming and breaking C-H bond distances that are the ordinate and abscissa for this plot. The C–H distances are varied from 1.22 to 1.38 Å with a grid spacing of 0.02 Å.
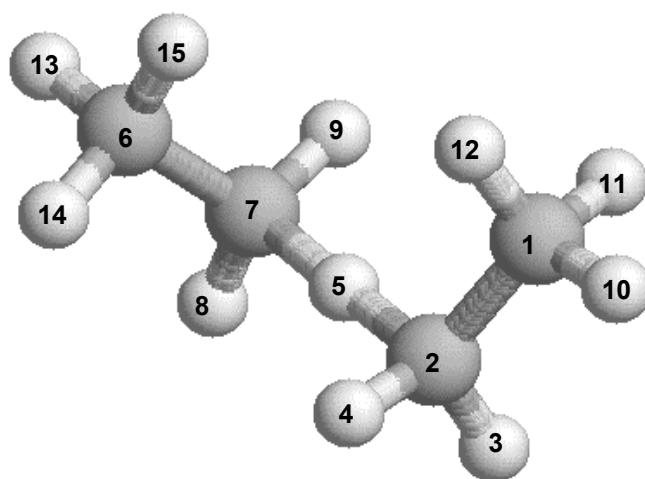
Figure 1

Figure 2